Postprint: Fine-Scale Analysis of Dry-Hot Wind Characteristics in Southern Xinjiang Region, 2020

Authors: Zulian Zhang

Date: 2022-01-26T17:59:39+00:00

Abstract

Using hourly reanalysis data at 5 km × 5 km resolution from the China Meteorological Administration Land Data Assimilation System (CLDAS) from May to July 2020, combined with crop development period data for the wheat planting areas in southern Xinjiang in 2020, we refined the definition of dry-hot wind based on hourly meteorological elements, compiled hourly dry-hot wind data for each grid point within the region, and analyzed the refined characteristics of light, moderate, and severe high-temperature low-humidity type and drought-wind type dry-hot winds in southern Xinjiang. The results show that: (1) The grid-point average days of light, moderate, and severe high-temperature low-humidity type and drought-wind type dry-hot winds in southern Xinjiang are 31.0 d, 13.8 d, 10.7 d, and 3.6 d, respectively; the grid-point average hours are 151.2 h, 54.6 h, 41.2 h, and 11.3 h, respectively. Ruoqiang, Hami, and the Turpan Basin are high-value areas for indicators such as dry-hot wind days, hours, and comprehensive intensity. (2) High-incidence days with regional high-temperature low-humidity type dry-hot wind average hours ≥ 6.5 h are concentrated in late June, early July, and mid-July. High-incidence days with regional drought-wind type dry-hot wind average hours ≥ 4.0 h mainly occur in May, mid-June, and early July. The affected area of high-temperature low-humidity type dry-hot wind reaches its maximum at 18:00 each day, while that of drought-wind type dry-hot wind reaches its maximum at 19:00. (3) In southern Xinjiang, the average frequencies of light, moderate, and severe high-temperature low-humidity type and drought-wind type dry-hot wind processes are 12.7, 7.9, 5.7, and 2.5 times, respectively, and the average maximum duration days of dry-hot wind processes are 8.4 d, 3.5 d, 2.7 d, and 1.2 d, respectively. The dry-hot wind in this region is characterized by extensive spatial coverage, high process frequency, and long process duration, necessitating sufficient attention to dry-hot wind defense.

Full Text

Preamble

Arid Zone Research (ChinaXiv Cooperative Journal) Vol. 39 No. 1, January 2022

Detailed Analysis of Dry-Hot Wind Characteristics in Southern Xinjiang in 2020

Authors: Zhang Zulian[1],[2], Mao Weiyi[1], Yao Yanli[2], Zhang Shanqing[2], Gu Yawen[2]

Affiliations:

1. Institute of Desert Meteorology, China Meteorological Administration, Urumqi, Xinjiang 830002, China
2. Xinjiang Xingnong Network Information Center, Urumqi, Xinjiang 830002, China

Abstract:

Using hourly reanalysis data from the China Meteorological Administration Land Data Assimilation System (CLDAS) at 5 km × 5 km spatial resolution from May to July 2020, combined with wheat growth stage data from southern Xinjiang, this study refines the definition of dry-hot wind based on hourly meteorological elements. Hourly dry-hot wind data were compiled for each grid point to analyze the detailed characteristics of light, moderate, and severe high temperature-low humidity type and dry wind type dry-hot wind in southern Xinjiang. The results show that: (1) The average grid-point cumulative days for light, moderate, and severe high temperature-low humidity type and dry wind type dry-hot wind were 31.0 days, 13.8 days, 10.7 days, and 3.6 days, respectively, while the average cumulative hours were 151.2 h, 54.6 h, 41.2 h, and 11.3 h. Ruoqiang, Hami, and the Turpan Basin represent high-value areas for dry-hot wind days, hours, and comprehensive intensity index. (2) Days with regional average duration $ $6.5 h for high temperature-low humidity type dry-hot wind were concentrated in late June, early July, and mid-July. Days with regional average duration $ $4.0 h for dry wind type dry-hot wind were concentrated in May, mid-June, and early July. During high-incidence periods, the largest affected area for high temperature-low humidity type occurred at 18:00, while the largest area for dry wind type occurred at 19:00. (3) The average process frequency for the four dry-hot wind categories was 10.7, 7.1, 5.7, and 2.9 times, respectively, with average maximum duration of 8.4 days, 3.5 days, 2.7 days, and 1.2 days. The extensive spatial coverage, high frequency, and long duration of dry-hot wind processes warrant serious attention for disaster prevention.

Keywords: wheat; dry-hot wind; detailed characteristics; southern Xinjiang

1 Data Sources and Methods

1.1 Data Sources

The study utilized hourly reanalysis data products from the China Meteorological Administration Land Data Assimilation System (CLDAS) at 5 km × 5 km resolution from May to July 2020. The CLDAS data integrate multi-source information from ground stations, satellites, and radar systems. The study area encompasses the region south of the Tianshan Mountains in Xinjiang, geographically bounded by 34.4°–45.05°N, 73.55°–96.35°E, comprising 30,000 grid points (Fig. 1). Among these, 29,992 grid points met the dry-hot wind criteria, with specific counts for each type: 29,992 for light high temperature-low humidity (HTLH_L), 29,992 for moderate (HTLH_M), 29,992 for severe (HTLH_H), and 2,546 for dry wind type.

Wheat development stage data for southern Xinjiang in 2020 show that spring wheat areas are primarily distributed in Turpan, Hami, Ruoqiang, Qiemo, and Yanqi Basin, while winter wheat areas are concentrated in Aksu, Kashgar, and Hotan regions. Mixed spring-winter wheat zones are found in Luntai, Korla, Ruoqiang, and Qiemo. The critical period from flowering to maturity for spring wheat mainly occurs from early May to mid-July (Table 1).

1.2 Dry-Hot Wind Classification Standards

According to the China Meteorological Industry Standard for wheat dry-hot wind disasters (QX/T 82-2019), dry-hot wind is classified as either high temperature-low humidity type or dry wind type, with the former further divided into three severity levels. The hourly identification criteria are:

1. **Severe high temperature-low humidity**: Temperature $\geq$ 35°C, relative humidity $\leq$ 25%, and wind speed $\geq$ 3 $\mathrm{m \cdot s^{-1}}$
2. **Moderate high temperature-low humidity**: Temperature $\geq$ 33°C, relative humidity $\leq$ 30%, and wind speed $\geq$ 3 $\mathrm{m \cdot s^{-1}}$
3. **Light high temperature-low humidity**: Temperature $\geq$ 30°C, relative humidity $\leq$ 30%, and wind speed $\geq$ 2 $\mathrm{m \cdot s^{-1}}$
4. **Dry wind type**: Temperature $>$ 25°C and wind speed $\geq$ 14 $\mathrm{m \cdot s^{-1}}$

1.3 Regional Dry-Hot Wind Day Index Calculation

Based on these standards, hourly meteorological elements at each grid point were evaluated for dry-hot wind conditions. Each hour meeting the criteria was counted as one dry-hot wind hour. Within the Beijing Time daily boundary (20:00–20:00), if a grid point accumulated n hours of dry-hot wind, it was recorded as a dry-hot wind day. The sum of dry-hot wind hours across all grid points on a given day was defined as the regional dry-hot wind day index (CID_1), expressed in hours. This index analyzes the daily evolution of regional dry-hot wind intensity during the study period. The calculation formula is:

$$\mathrm{AVGH} = \frac{\sum_{i=1}^{N_A} h_i}{N_A}$$

where AVGH represents the daily average duration of dry-hot wind at grid points, h_i denotes the hourly count for each grid point, and N_A is the total number of grid points experiencing dry-hot wind that day.

1.4 Regional Dry-Hot Wind Comprehensive Intensity Index Calculation

Building upon previous research on comprehensive intensity indices for high temperature-low humidity dry-hot wind, this study designed a regional comprehensive intensity index (CID) for southern Xinjiang. The formula is:

$$I_{xj} = (T_{xj} - T_c) \times (R_c - R_{xj}) \times (V_{xj} - V_c)$$

$$\mathrm{CID}_x = \sum_{j=1}^{n} I_{xj}$$

$$\mathrm{CID}_1 = \sum_{x=1}^{m} \sum_{j=1}^{t} I_{xj}$$

where I_{xj} is the comprehensive intensity index for grid point x at hour j; T_c, R_c, and V_c are threshold values based on light high temperature-low humidity criteria (30°C, 30%, and 2 $\mathrm{m \cdot s^{-1}}$, respectively); T_{xj}, R_{xj}, and V_{xj} are observed temperature, relative humidity, and wind speed; n is the total dry-hot wind hours at grid point x; CID_x represents the cumulative intensity for grid point x; m is the number of grid points affected on a given day; and t is the hourly count for each grid point. CID_1 reflects the regional comprehensive intensity for spatial and temporal analysis.

---

2 Results and Analysis

2.1 Spatial Distribution of Dry-Hot Wind Days and Hours

The duration and spatial extent of dry-hot wind reflect its intensity and hazard level—more days and hours over larger areas indicate greater damage potential. In southern Xinjiang, high temperature-low humidity dry-hot wind occurs below 1500 m elevation, while dry wind type is concentrated in the Turpan Basin' s Thirty Mile Wind Zone, Hami' s Hundred Mile Wind Zone, and the Tieganlike area in Bayingolin.

As shown in Fig. 2 and Table 2, the ranges for light, moderate, severe, and dry wind type were 1–88 days, 1–87 days, 1–86 days, and 1–36 days, respectively, with grid-point averages of 31.0 days, 13.8 days, 10.7 days, and 3.6 days. Corresponding hour ranges were 1–1098 h, 1–902 h, 1–832 h, and 1–242 h, with averages of 151.2 h, 54.6 h, 41.2 h, and 11.3 h.

Based on light high temperature-low humidity day counts (HTLH_L), the region was divided into five intensity grades: I_1 (1–10 days), II_1 (10–20 days), III_1 (20–30 days), IV_1 (30–60 days), and V_1 (>60 days). Grade I_1 covered 3,939 grid points (13.1% of affected area), mainly in Aksu. Grade II_1 comprised 4,737 grid points (15.8%), distributed in eastern Xinjiang and the Turpan southern region at 200–600 m elevation, as well as Aksu, Kashgar, and Hotan at 1200–1500 m. Grade III_1 included 7,591 grid points (25.3%) across the Tarim Basin (1000–1200 m), Tarim River basin (800–1000 m), and parts of Kashgar. Grade IV_1 accounted for 11,558 grid points (38.5%) extending from Hongliuhe to Tieganlike, and north of the Tarim River to Yuli, Luntai, and Qiemo. Grade V_1 contained 2,099 grid points (7.0%) in Ruoqiang, Hami, and Turpan basins.

In Grade I_1 (primary winter wheat zone), average days/hours were 5.2/11.6 for light, 1.5/2.0 for moderate, 1.4/1.5 for severe, and 2.5/4.2 for dry wind type. The most intense Grade V_1 showed averages of 71.4 days/563.8 hours (light), 50.2 days/290.4 hours (moderate), 43.3 days/235.6 hours (severe), and 4.9 days/17.3 hours (dry wind type).

2.2 High-Incidence Periods

Understanding the timing and evolution of dry-hot wind is crucial for effective defense. During May–July 2020, southern Xinjiang experienced extensive dry-hot wind with high temporal concentration. Eleven days had regional total hours $ 10^{4}$ h or affected grid points $ 2×10^{4}$, mainly in early and late June and early and late July. Seven days had regional average duration $ $6.5 h for high temperature-low humidity type, concentrated in late June, early July, and mid-July. Seven days had regional average duration $ $4.0 h for dry wind type, occurring in May, mid-June, and early July (Table 3). This period coincides with the milk-ripe stage of wheat in Hami, Yanqi, Hotan, Kashgar, and Aksu.

Within high-incidence days, the spatial coverage peaked during 17:00–20:00. At 18:00, high temperature-low humidity type reached maximum extent with 591,749 light, 204,384 moderate, and 145,175 severe grid points. Dry wind type peaked at 19:00 with 2,546 affected grid points (Fig. 3d).

2.3 Spatial Distribution of Dry-Hot Wind Processes

A dry-hot wind process is defined as consecutive days meeting the criteria at a grid point. Processes lasting 2 days can damage local fields; 3–4 days affect 1/3–1/2 of fields; 5–9 days cause widespread damage; and >10 days lead to

universal withering. Process frequency and maximum duration were analyzed using light high temperature-low humidity process counts (HTLH_L), divided into four grades: I_2 (1-5 processes), II_2 (5-10), III_2 (10-15), and IV_2 (>15).

Process frequencies ranged from 1-24 times (light), 1-22 (moderate), 1-21 (severe), and 1-19 (dry wind type), with averages of 10.7, 7.1, 5.7, and 2.9 times, respectively. Maximum duration ranged from 1-53 days, 1-46 days, 1-46 days, and 1-5 days, with averages of 8.4 days, 3.5 days, 2.7 days, and 1.2 days (Fig. 4, Table 4).

Grade I_2 covered 12.9% of affected grid points in Hongliuhe-Turpan south and Aksu. Grade II_2 comprised 22.2% in Hotan and Kashgar. Grade III_2 represented 60.8% across Hami, Turpan, Tieganlike, Ruoqiang, and both sides of the Tarim River. Grade IV_2 accounted for 4.1% in scattered locations. In Grade II_2, average process frequency/duration were 8.4 times/9.0 days (light), 5.5/3.5 (moderate), 5.5/3.4 (severe), and 3.2/1.4 (dry wind type), indicating potential local damage without defense. The most severe Grade IV_2 showed averages of 16.6 times/7.4 days (light), 8.0/3.1 (moderate), 5.8/2.4 (severe), and 3.8/1.3 (dry wind type), suggesting severe widespread damage under unprotected conditions.

2.4 Spatiotemporal Distribution of Regional Comprehensive Intensity Index

Using the comprehensive intensity index CID, four grades were established: I_3 (1-10), II_3 (10-20), III_3 (20-60), and IV_3 (60-372). Grade I_3 covered 28.3% of grid points (average CID = 4.5) in Hotan, Kashgar, and Aksu. Grade II_3 comprised 23.5% (CID = 14.6) in Bayingolin and parts of Aksu and Kashgar. Grade III_3 represented 32.6% (CID = 34.7) in southern Bayingolin. Grade IV_3 accounted for 15.6% (CID = 107.0) in Hami, Turpan, Hongliuhe-Tieganlike, Ruoqiang, and Qiemo (Fig. 5).

During May-July 2020, regional daily CID_1 $\geq$ 1.32 occurred on 11 days, mainly in early June, late June, early July, and mid-July. CID_1 $\geq$ 1.4 appeared on 7 days, concentrated in late June and early-mid July. The distribution of regional average duration $\geq$ 6.5 h closely matched CID_1 $\geq$ 1.32 patterns, while duration $\geq$ 5.7 h aligned with CID_1 $\geq$ 1.4 patterns (Table 5).

---

3 Discussion

Southern Xinjiang' s arid climate makes it a dry-hot wind-prone region. The impact on wheat grain filling and yield depends on timing, intensity, frequency, microclimate conditions, and wheat resistance capacity. Disaster risk results from combined effects of meteorological hazard, exposure, vulnerability, and mitigation capacity. Local farmers have implemented protective measures: (1)

planting early-maturing, stress-resistant varieties; (2) rational irrigation to maintain soil moisture; (3) foliar fertilization during late growth stages; and (4) establishing shelterbelts. Since 2010, unified water resource management in the Tarim River basin has improved ecological security, enhanced shelterbelt construction, and effectively mitigated natural disasters. These measures have significantly improved defense capabilities, meaning strong dry-hot wind events may not necessarily cause substantial yield losses.

---

4 Conclusions

Based on high-resolution CLDAS reanalysis data, this study analyzed detailed dry-hot wind characteristics in southern Xinjiang during May–July 2020:

1. **Severe dry-hot wind hazard**: The region experienced predominantly high temperature-low humidity type dry-hot wind below 1500 m elevation, with dry wind type also severe in Turpan's Thirty Mile Wind Zone, Hami's Hundred Mile Wind Zone, and Bayingolin's Tieganlike area. Average grid-point cumulative days/hours were 31.0 days/151.2 h (light), 13.8 days/54.6 h (moderate), 10.7 days/41.2 h (severe), and 3.6 days/11.3 h (dry wind type).
2. **High-incidence timing**: Regional average duration $ $6.5 h for high temperature-low humidity type occurred on 7 days (late June, early-mid July). Dry wind type average duration $ $4.0 h occurred on 7 days (May, mid-June, early July). Daily peak coverage occurred at 18:00 for high temperature-low humidity type and 19:00 for dry wind type.
3. **Process characteristics**: Average process frequencies were 10.7, 7.1, 5.7, and 2.9 times, with maximum durations of 8.4, 3.5, 2.7, and 1.2 days. The high frequency and long duration of processes can cause severe damage without protective measures.

These findings provide technical support for precise agricultural disaster prevention and risk reduction strategies for wheat and other crops in southern Xinjiang.

References

[1] Northern Wheat Dry Hot Wind Research Cooperation Group. *Dry Hot Wind of Wheat*. Beijing: Meteorological Press, 1988.

[2] Hou Qi, Zhang Bo, He Hang, et al. Spatiotemporal variation of dry hot wind events in the Hexi region in recent 50 years. *Arid Zone Research*, 2019, 36(2): 403-411.

[3] Huo Zhiguo, Shang Ying, Wu Dingrong, et al. Review on disaster of hot dry wind for wheat in China. *Journal of Applied Meteorological Science*, 2019, 30(2): 129-141.

[4] Chen Yongchuan, Liu Liyuan, Ban Haifeng. Harm of dry hot wind to grape florescence and its defense methods. *Xinjiang Agricultural Science and Technology*, 2020, 42(6): 9.

[5] Zhao Huarong, Ren Sanxue, Qi Yue, et al. Defensive effect of irrigation at different stage on hot dry wind stress on winter wheat. *Agricultural Research in the Arid Areas*, 2019, 37(4): 58-65.

[6] Deng Zhenyong, Zhang Qiang. Impact of climate warming and drying on dry hot wind in the North of China. *Journal of Glaciology and Geocryology*, 2009, 31(4): 664-671.

[7] Yang Tao. Numerical Simulation of the Effects of Irrigation on Regional Climate in Tarim Basin, Xinjiang. Yangling: Northwest A & F University, 2020.

[8] Ma Guangxu. Analysis of climatic conditions for spring wheat planting in Yanqi Hui Autonomous County, Xinjiang. *Journal of Agricultural Catastrophology*, 2020, 10(3): 97-98.

[9] Chen Ying, Shao Weiling, Cao Meng, et al. Variation of summer high temperature days and its affecting factors in Xinjiang. *Arid Zone Research*, 2020, 37(1): 58-66.

[10] Li Seng, Han Lijuan, Guo Andong, et al. Spatial-temporal characteristics of dry hot wind for winter wheat in Huang-Huai-Hai region from 1961 to 2015. *Acta Ecologica Sinica*, 2018, 38(19): 6972-6980.

[11] Li Sen, Han Lijuan, Zhang Lei, et al. Spatial-temporal characteristics of dry hot wind factors in Huang-Huai-Hai region. *Journal of Natural Disasters*, 2020, 29(1): 183-192.

[12] Li Tongxiao, Cheng Lin, Ma Qingrong. Occurrence regularity of dry hot wind and relationship with winter wheat flowering period in Henan Province. *Hubei Agricultural Sciences*, 2019, 58(22): 58-64.

[13] Cheng Lin, Zhang Zhihong, Shi Guifen, et al. Flux characteristics of wheat field under dry hot wind weather condition. *Journal of Arid Meteorology*, 2020, 38(2): 205-212.

[14] La Yongchang, Li Lipin, Zhang Lei. Spatial and temporal characteristics of dry hot wind disaster for spring wheat in the irrigated areas of Ningxia. *Journal of Triticeae Crops*, 2016, 36(4): 516-522.

[15] Ma Yali, Luan Qing, Li Weiwei, et al. Distribution characteristics of dry hot wind and its effect on yield of winter wheat in Shanxi Province. *Journal of Shanxi Agricultural Sciences*, 2017, 45(7): 1134-1138.

[16] Zhang Cuiying, Fan Jinghao, Zhang Bin. Dry hot wind characteristic and statistical forecasting model in Southwest of Shandong Province. *Journal of Arid Meteorology*, 2016, 34(1): 207-211.

[17] Han Lijuan, Zhao Xiaofeng, Zhang Lei. Analysis of meteorological conditions and their impacts on the growth period of grain and oil crops in the summer of 2020. *Chinese Journal of Agrometeorology*, 2020, 41(9): 605-607.

[18] Yang Zhijie, Jin Linxue, Wu Rongsheng, et al. Refined risk division of dry hot wind disaster for spring wheat in Inner Mongolia based on GIS. *Journal of Arid Meteorology*, 2019, 37(5): 866-872.

[19] Huo Zhiguo, Shang Ying, Wang Chunzhi, et al. *Disaster Grade of Dry Hot Wind for Wheat (QX/T 82-2019).* Beijing: China Meteorological Administration, 2019.

[20] Wang Chunyi, Pan Yaru, Ji Guishu. Index analysis of dry hot wind year' s type and forecasting model in Shijiazhuang district. *Acta Meteorologica Sinica*, 1991, 49(1): 104-107.

[21] Li Sen, Han Lijuan, Mao Liuxi, et al. A modified comprehensive intensity index of dry-hot wind hazard for wheat. *Journal of Natural Disasters*, 2018, 27(2): 174-182.

[22] Li Mengyi, Deng Mingjiang, Ling Hongbo, et al. Evaluation of ecological water security and analysis of driving factors in the lower Tarim River, China. *Arid Zone Research*, 2021, 38(1): 39-47.

[23] Shen Fangyu, Wang Yonghong, Li Shengyu, et al. Study on soil aggregates of the desert highway shelterbelt in Tarim. *Arid Zone Research*, 2015, 32(5): 910-917.

[24] Sun Lin, Mu Guijin, Zhou Jie, et al. Seasonal variation of shelterbelt porosity of *Populus alba* pyramidalis at the edge of Cele Oasis in the south of Tarim Basin. *Arid Zone Research*, 2015, 32(6): 1181-1185.

Figures

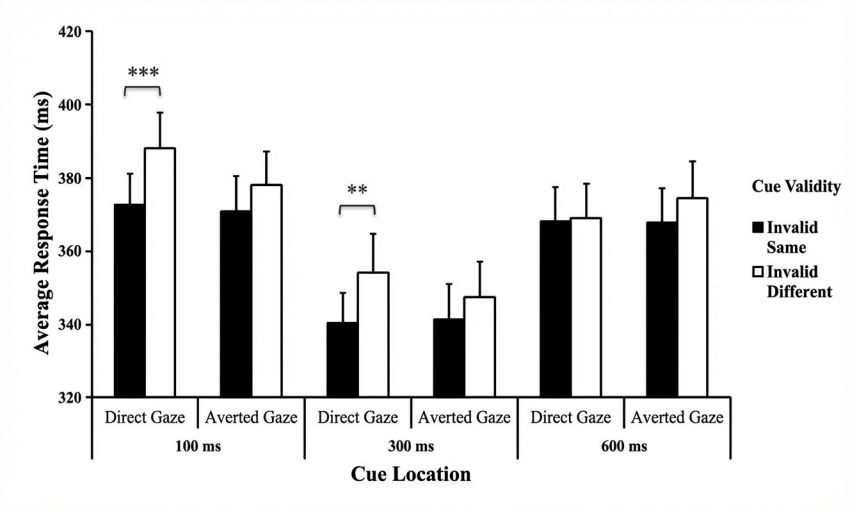

Figure 1: Figure 1

Figure 2: Figure 3

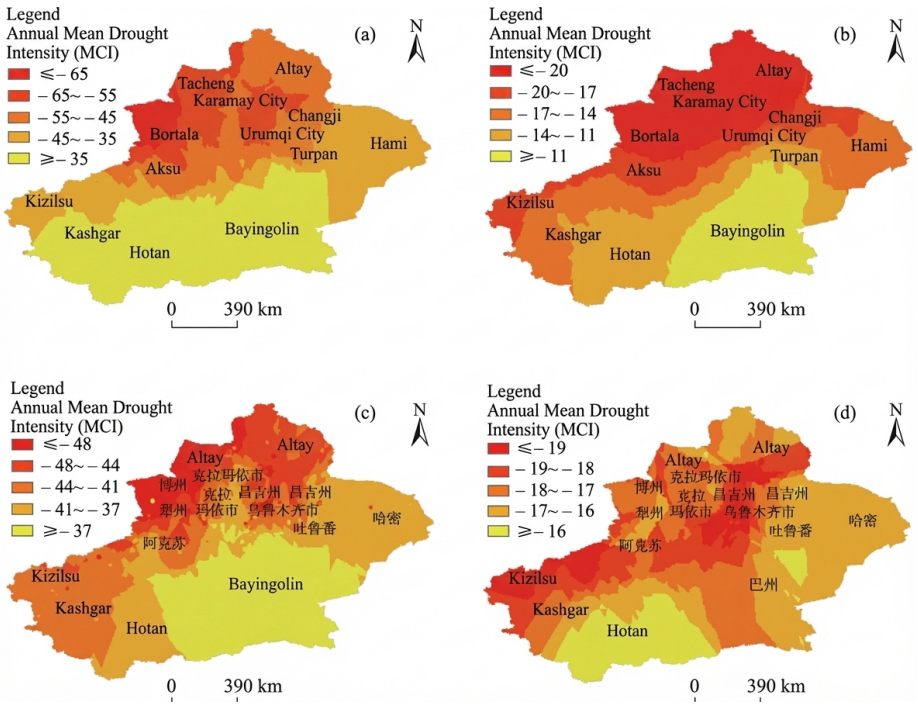

Figure 3: Figure 5